

Optical coherence tomography technology for diagnosis of diseases in organs

Su Li¹, Song Kaiwen², Lv Peitong², Wang Haoran², Sun Mingyang², Zhang Xiaotong², Zhang Tianyu^{2*}

(1. Jilin Provincial Institute of Education, Changchun 130022, China;

2. Key Laboratory of Geophysical Exploration Equipment, Ministry of Education, College of Instrumentation & Electrical Engineering, Jilin University, Changchun 130061, China)

Abstract: In modern medicine, nuclear scans, Positron Emission Tomography (PET), and Magnetic Resonance Imaging (MRI) technology have been widely used to provide tissue morphology and functional information. However, these technologies have their own shortcomings in resolution or imaging depth. A new optical detection technology based on the principle of low-coherence interference can achieve high-resolution and large-depth imaging at the same time. This technology is called optical coherence tomography (OCT) technology. OCT technology is a non-contact, non-invasive, non-damage imaging technology that combines high longitudinal resolution with high transverse resolution, and can achieve the same effect as biopsy observation. OCT uses a low-energy near-infrared light source as the detection light, combined with non-damaging methods such as microscope heads, hand-held probes or endoscopes, for routine detection, and will not cause damage to biological tissues. At the same time, OCT combined with rapidly developing image acquisition, analysis and processing technology can realize real-time three-dimensional imaging, and extract useful information for diagnosis for quantitative analysis, which provides convenience for doctors' diagnosis. This review focuses on the classic OCT imaging technology and its related medical application technologies, such as SD-OCT, SS-OCT, aOCT, PS-OCT and D-OCT, in the detection of diseases of the respiratory system, oral cavity, brain tissue, kidney and other major organs in the application.

Key words: optical coherence tomography; respiratory system; airway diseases; oral cancer

CLC number: T19 **Document code:** A **DOI:** 10.3788/IRLA20210803

光学相干层析成像技术在器官疾病诊断上的应用

苏 李¹, 宋凯文², 吕沛桐², 王浩然², 孙铭阳², 张晓彤², 张天瑜^{2*}

(1. 吉林省教育学院, 吉林 长春 130022; 2. 吉林大学 仪器科学与电气工程学院 地球物理勘探装备教育部重点实验室, 吉林 长春 130061)

摘 要: 在现代医学中,核扫描、正电子发射断层扫描 (Positron Emission Tomography, PET) 和磁共振成像 (Magnetic Resonance Imaging, MRI) 技术已被广泛应用于提供组织形态和功能信息。但是这些技术在分辨率或成像深度上各有缺点,而一种基于低相干干涉原理的新型光学检测技术则可以同时实现高分辨率和大深度成像,该技术称为光学相干层析成像技术 (Optical Coherence Tomography, OCT)。OCT 技术是一种将高纵向分辨率和高横向分辨率结合的非接触、非侵入、无损影像技术,可以实现

收稿日期:2021-12-20; 修订日期:2022-02-25

基金项目:国家重点研发项目 (YFC 0409105); 中国吉林省科技厅项目 (20210204193 YY); 沈阳科技计划公共卫生研发专项 (21-172-9-18)

作者简介:苏李,男,讲师,硕士,主要从事电子信息工程等方面的研究。

通讯作者:张天瑜,男,副教授,博士生导师,博士,主要从事光纤传感等方面的研究。

与活体组织病理学观察相同的作用。OCT 采用低能量的近红外光源作为探测光,并结合显微镜头、手持式探头或内窥镜等非损伤方式进行常规检测,不会对生物组织造成损伤。同时 OCT 结合发展迅速的图像采集分析处理技术,可实现实时三维成像,从中提取对诊断有用的信息进行定量分析,为医生的诊断提供便利。该综述重点介绍经典 OCT 成像技术及其相关医疗应用技术,如 SD-OCT、SS-OCT、aOCT、PS-OCT 和 D-OCT,在呼吸系统、口腔、脑组织和肾脏等其他主要器官疾病检测中的应用。

关键词: 光学相干层析成像; 呼吸系统; 气道疾病; 口腔癌

0 Introduction

Imaging modalities, such as X-ray computed tomography (CT), magnetic resonance imaging (MRI), and ultrasound imaging have been used as clinical diagnosis tools for many organ structures. In the airway, X-ray cephalometry and CT can obtain structural information. However, the availability, cost, and risk of ionizing radiation related to those imaging techniques have hindered their applications for daily screening and monitoring^[1]. Oral and skin cancer are prevalent and pose considerable health care problems worldwide^[2]. Visual examination by physicians has limited the opportunity to manage diseases in the early stage because of high inter- and intra-observer errors. In internal organs like kidneys, the brain, bowels and gastro-intestines, medical imaging techniques such as nuclear scans, PET and MRI can detect morphological and functional abnormalities. However, the clinical utility of these techniques are limited by their high cost, lack of availability, and difficulty associated with operation during surgery^[3].

Optical coherence tomography (OCT) is suitable for diagnosing diseases in a clinical and surgical setting. OCT is a low-coherence interferometric technique used as an optical analog to ultrasound^[4] that exhibits higher imaging speed and spatial resolution than CT and X-ray. Axial and transverse resolutions of a typical OCT imaging is 10-20 microns and typically determined by the bandwidth of the light source and numerical aperture of collimator. By using ultrabroad bandwidth sources, such as supercontinuum light sources and solid-state lasers and femto-second laser, the axial resolution can be improved to a few microns. With enhanced transverse resolution, a detailed tissue structure up to a few microns can be visualized. Moreover, OCT provides depth-resolved images of biological tissues of up to -2 mm beneath the

tissue surface^[4]. At present, pathology is the gold standard for many disease diagnoses. With the advancement of an accurate noninvasive optical imaging technique such as OCT, tissue biopsies and processing for medical diagnosis can potentially be eliminated and benefit treatment planning by achieving an easier bedside diagnosis^[5].

This work reviews the different applications of OCT, focusing on obstructive sleep apnea (OSA) in airway diseases, oral cancer in oral diseases, cerebral edema in brain tissues, renal cell carcinoma in renal diseases, and colon cancer in gastrointestinal diseases.

1 OCT in airway applications

Respiratory disease and dysfunction in the airway affect the patient's quality of life. OCT imaging has been demonstrated to be a viable intra-operative tool. Similarly, the oral region is a vulnerable area of the body, and OCT allows non-invasive monitoring of oral cells. The application of OCT in the airway and oral cavity will be reviewed in the following sections.

Airway injury is frequently caused by endotracheal intubations, long-term tracheostomies, trauma, airway burns, and some systemic diseases^[6]. Due to the rapid progression of airway injury and decreased survival rate over time, a rapid and less invasive technique for both early assessment and interventional treatment of acquired airway stenosis is needed^[7].

OCT can delineate microstructures, such as epithelium, mucosa, cartilage, and glands, in all samples^[8] and identify the epithelium and lamina propria while providing detailed structural information on normal and diseased tissues^[9]. A reliable means to noninvasively image living tissues at a high resolution could significantly help the diagnosis, treatment, and monitoring of diseases within the lower aerodigestive tract.

The use of OCT assesses the engraftment of

exogenous adipose stem cells in injured tracheal epithelium with fluorescent microscopy and detects and monitors the degree of airway injury in the same tracheal epithelium. This method can further contribute to the study of immunomodulatory effects of adipose-derived stromal/stem cells (ASCs) in airway stenosis.

1.1 Airway

The application of OCT in the upper airway includes the detection of obstructive sleep apnea (OSA) and subglottic and nasal diseases. Measurement of airway thickness and three-dimensional imaging of the respiratory tract can be conducted to display the respiratory tract model and solve upper respiratory disease problems. The following is a review of OCT application in the upper airway.

1.1.1 Obstructive sleep apnea (OSA)

Obstruction of the upper airway can adversely affect breathing and gas exchange, especially during sleep. OSA is characterized by the repetitive closure of the upper airway during sleep^[10] and affects an estimated 12 to 18 million Americans from every age group^[11]. OSA among adults is characterized by dynamic collapse and reduces airflow^[12]. Measuring the upper airway dimension, such as caliber and volume, can reveal pathophysiology of airway collapse during sleep. The use of functional OCT imaging, such as long-range OCT (LR-OCT) and anatomical OCT (aOCT), has the unique advantage of allowing dynamic measurements during sleep and enabling direct measurement of the effect of treatments on airway caliber. Furthermore, OCT can be incorporated into a small endoscopic imaging probe to generate quantitative and real-time images of the upper airway inside the patient that enable an accurate determination of shape and size^[10]. A new LR-OCT system integrates high-speed imaging with real-time position tracking to generate an accurate 3D anatomical structural model of the human upper airway. The system can achieve rapid and complete visualization and quantification of the airway which can then be used in computational simulations to determine obstruction sites^[13].

Sharma et al. showed LR-OCT can immediately image the upper airway of children under general anesthesia before and after tonsillectomy and adenoidectomy^[14]. This study investigated the feasibility of using

LR-OCT to identify both normal anatomy and narrowing airway sites and quantitatively compare the pre- and postoperative airway lumen size in the oropharyngeal and nasopharyngeal regions. The volumetric rendering of pre- and postoperative images clearly showed regions with airway collapse and postsurgical improvement in airway patency^[15]. Figure 1 shows the LR-OCT imaging of the upper airway. Figure 2 shows the axial aOCT imaging of the nasopharynx post adenoidectomy before and after surgery.

The frequency-domain optical delay line (FDODL) was developed for ultrafast laser pulse autocorrelation and subsequently used in OCT systems for group- and phase-delay scanning to achieve high frame rates required for artifact-free OCT imaging^[1]. A section of the upper airway and esophagus was shown with a radial scanning

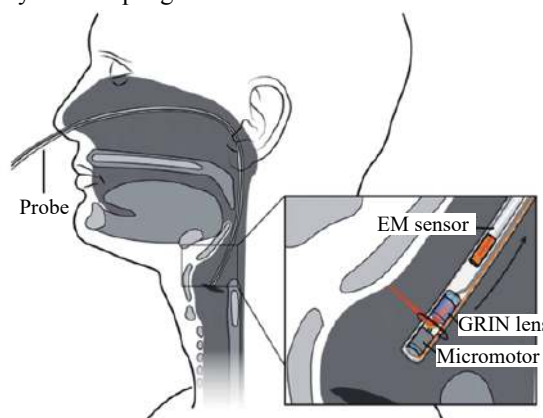


Fig.1 LR-OCT imaging of the upper airway
Pre-operative OCT Post-operative OCT

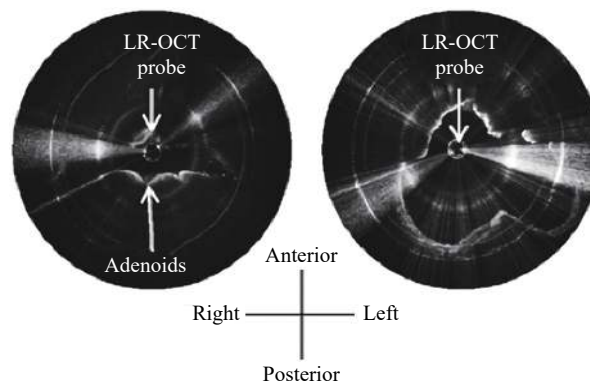


Fig.2 Preoperative axial OCT image of the nasopharynx and adenoids of a 7 year old male patient (left image). Postoperative axial OCT image of the nasopharynx of the same patient (right image)(Note: The adenoids have been removed and the airway lumen is larger^[15])

range of 26 mm. This imaging was the first attempt to obtain in vivo size and shape measurements of the human upper airway by using catheter-based OCT. The results showed that substantial segments of organ circumferences could be detected to provide medically useful infor-

mation^[1]. Figure 3 shows in vivo measurements of six different anatomical locations in the upper respiratory and digestive tracts where five images were taken at different locations along the airway from the nasal cavity to the hypopharynx, and one image was obtained in the esophagus.

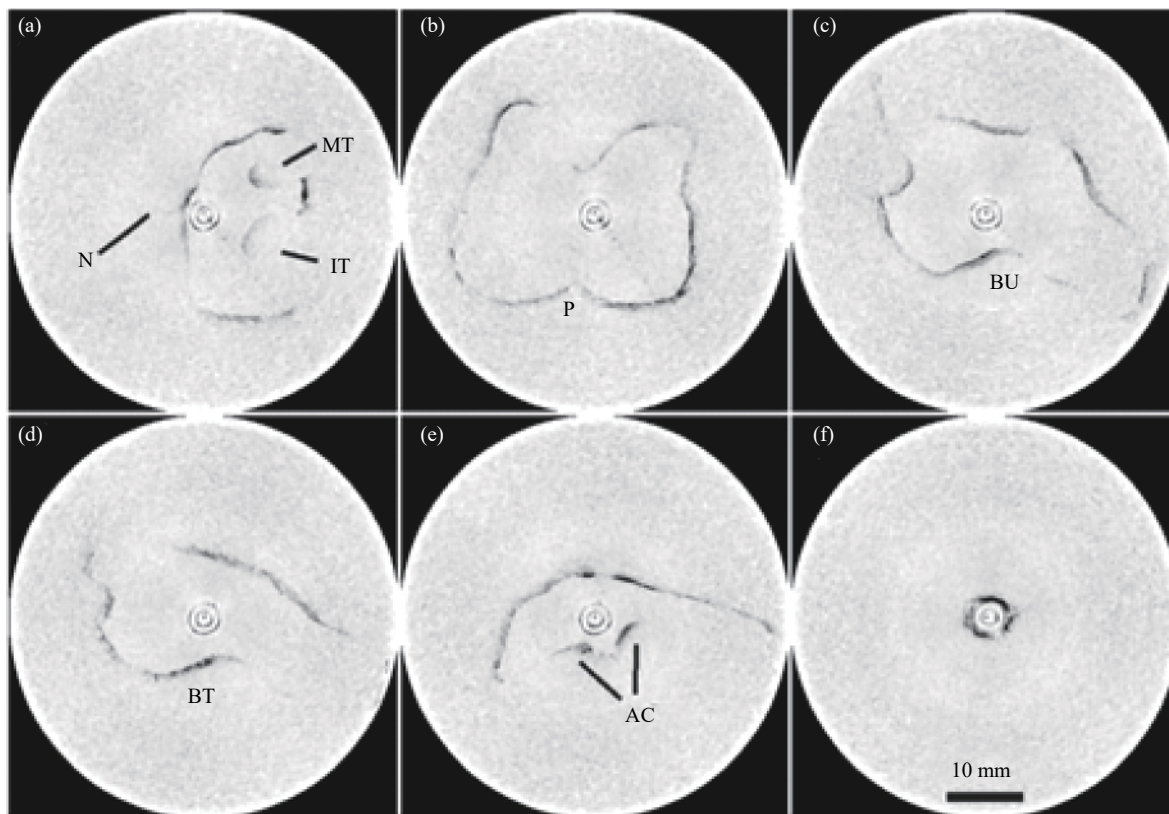


Fig.3 Six in vivo measurements of the airway (and esophagus) of a human and arranged by distance in the airway: (a) nasal cavity, (b) nasopharynx, (c) velopharynx, (d) oropharynx, (e) hypopharynx, and (f) esophagus. (Note the following anatomical features: nasal septum (N), middle turbinate (MT), inferior turbinate (IT), posterior nasal spine (P), base of uvula (BU), base of tongue (BT), and arytenoid cartilage (AC). The two circles at the center of the images are the reflections from the inner and outer surfaces of the catheter^[1])

By using aOCT, the airway cross-sectional area (CSA) and the anteroposterior (AP) and lateral diameters were obtained from velopharyngeal regions. The shapes, sizes, and lengths of the pharyngeal airway in individuals with and without OSA were compared. Relative to healthy controls, the velopharyngeal CSA was approximately 40% less than those with OSA. Figure 4 shows that several landmarks are readily identifiable from the aOCT images of the upper airway.

In addition, aOCT can resolve dynamic changes in airway size and shape due to external factors, such as applied air pressure^[17]. The effect of soft palate

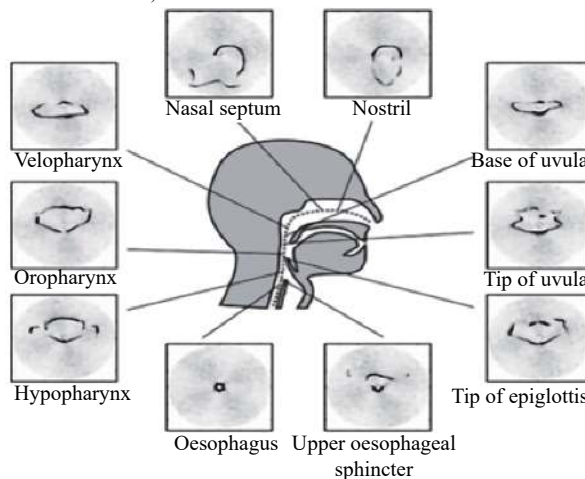


Fig.4 Various anatomic landmarks and regions of the pharynx from the upper esophagus and completed in one nostril^[16]

displacement and sidewall deformation on the velocity and pressure fields has been studied. A complete and accurate flow and pressure fields for an individual could be generated^[11].

The minimally invasive imaging of upper airway obstructions was necessary to improve clinical decision-making^[18]. Swept-source anatomical OCT (SS-aOCT) has been used for upper airway luminal imaging to demo-

nstrate accurate 3D luminal reconstructions of human airway phantoms and ex vivo swine trachea. This method could provide unprecedented dynamic airway imaging and obtain new insight into obstructive breathing disorders in conjunction with computed fluid dynamic (CFD) analysis. Figure 5 presents a comparison of the aOCT results of imaging an ex vivo swine airway with a high-resolution CT scan on the same tissue.

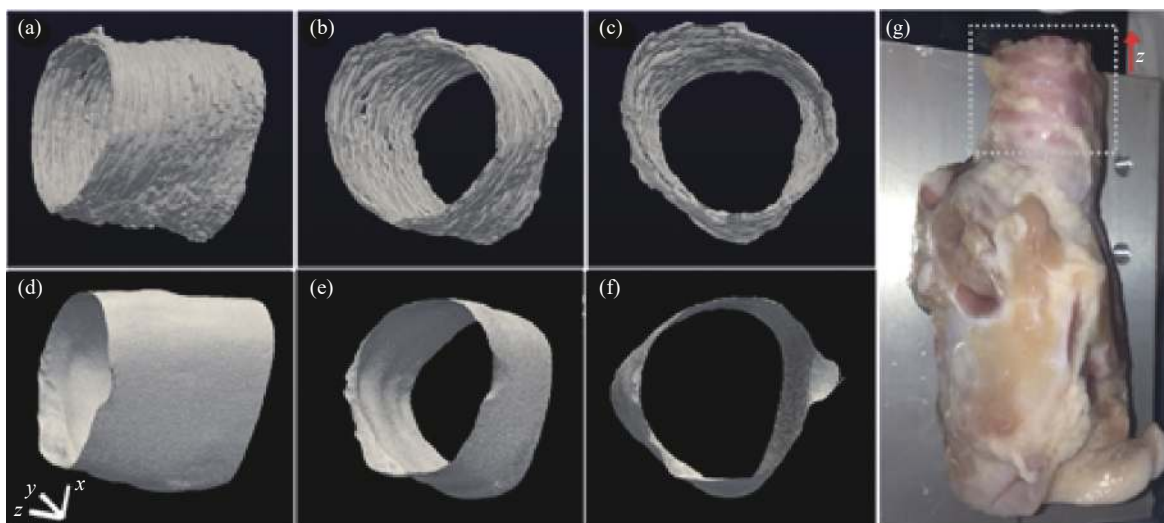


Fig.5 (a)–(c) aOCT images of swine trachea displayed in three different viewing angles; (d)–(f) Corresponding CT images; (g) Photograph of the swine airway. (Note: The imaged region is indicated by the dotted square. The x , y , and z scale bars each represent 3 mm)

1.1.2 Subglottic microanatomy

At present, no imaging modality allows in vivo characterization of subglottic microanatomy to identify early signs of subglottic stenosis (SGS) while a child remains intubated. FD-OCT has been applied to the serial monitoring of neonatal subglottic in long-term intubated infants who are at risk of acquiring SGS^[19]. Long-range FD-OCT produces high-resolution 3D volumetric images of the pediatric subglottic. Identifying occult subepithelial pathology of the subglottic could help neonatologists in managing the airway and reducing the incidence of subglottic ulceration and scarring^[19]. Figure 6 shows the intraoperative FD-OCT of the pediatric airway, and Figure 7 presents the subglottic OCT image of the same patient.

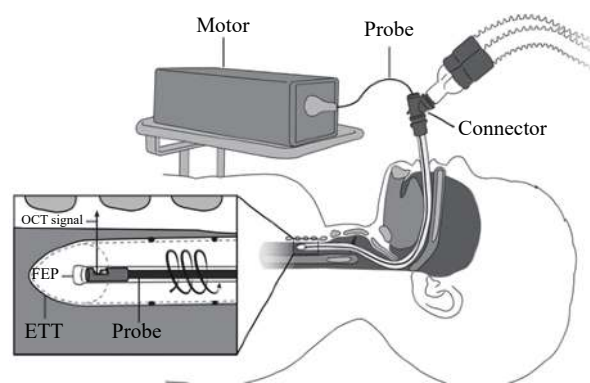


Fig.6 Intraoperative FD-OCT of the pediatric airway. Note: A 0.7 mm OD OCT probe (75–80 cm length) is connected to a combined rotational motor and dual-motor stage for linear pullback. The probe, housed in a transparent fluorinated ethylene propylene sheath, is inserted through a Y-connector and pushed inside the endotracheal tube. The combined motors simultaneously rotate and retract the probe through the upper airway as the OCT signal is reflected at 90° into the tissue. ETT = endotracheal tube^[19]

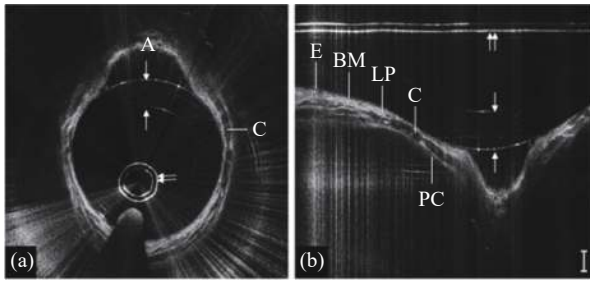


Fig.7 OCT image of pediatric subglottis represented in (A) polar coordinates and (B) cropped segment of Cartesian coordinates. (Note: A: anterior, C: cricoid cartilage, E: epithelium, BM: basement membrane, LP: lamina propria, PC: perichondrium, double arrows: probe sheath, and single arrow: endotracheal tube inner/outer wall. Bar = 500 μm ^[19])

1.1.3 Airway remodeling and asthma

The structural changes and thickening of the airway wall components that occur in individuals with chronic respiratory diseases, also known as airway remodeling, are responsible for many of the adverse outcomes associated with this type of diseases^[20].

Adams et al. have developed polarization-sensitive OCT (PS-OCT) combined with an endoscopic imaging probe to detect smooth muscle structure and function in asthmatic patients^[21]. PS-OCT can visualize tissue with high birefringence and quantify the local retardation of polarized light. Airway smooth muscle remodeling is known to occur in asthmatic patients, and this study has provided the first in vivo insights into the mechanism of remodeling in humans.

1.1.4 Smoke and chemical-induced airway injury

The diagnosis of inhalation injury is a primary unresolved problem in modern burn care^[22]. Imaging the subsurface structure of the airway wall is important in detecting abnormalities during airway injuries. Smoke exposure and inhalation risks, including thermal, toxic, and chemical injuries, result in airway hyperemia, edema, sloughing, and necrosis. The pathophysiological information, such as mucosal thickness, mucus secretion, and airway lumen deformation in the injured airway wall, could provide early diagnosis and prediction of respiratory diseases^[23]. The airway thickness measured in OCT increased in sheep and pigs after smoke inha-

lation^[24]. Additionally, smoke inhalation injury is frequently accompanied by cyanide poisoning and acute respiratory distress syndrome that can result in increased morbidity and mortality. Currently, a method to quantitatively determine the extent of airway injury is lacking.

There is an improved LR-OCT system with an up to 25-mm imaging range that demonstrates the feasibility of using our LR-OCT system to qualitatively and quantitatively assess the progression of smoke inhalation injury over time. Using LR-OCT, the technology can achieve real-time near histology grade evaluation of airways that could be useful for rapid non-invasive assessment of inhalation injury^[22]. The LROCT system showed excellent capability for monitoring changes of airway thickening over time and tracked progressive thickening of the airway mucosa as the injury progressed.

The quantification of acute and long-term thickness changes of the mucosal area in the airway by using in vivo 3D endoscopic OCT could provide a sensitive tool for investigating the effectiveness of various therapeutic interventions in smoke inhalation and other airway injuries^[24]. Figure 8 shows a representative in vivo image of a normal rabbit airway with corresponding histology.

Cystic fibrosis (CF) can lead to chronic inflammation and the remodeling of airways. However, information on the associated mucosal microanatomical changes is limited^[6]. Therefore, the potential of OCT in the in vivo imaging of the upper airway mucosa in CF patients was studied. OCT images could present mucosal details. The mean nasal mucosa and epithelial layer thickness increased in CF. The structural changes of the nasal mucosa were associated with long- and short-term antibiotic treatments and raised IgE levels. In CF patients, antibiotic therapy was associated with reduced nasal mucosa thickening^[6].

To investigate whether OCT could differentiate between the composite microstructural layers of the human airway and simultaneously determine in situ morphologic changes, a study obtained cross-sectional images of bronchi from 15 patients undergoing lung resections for cancer by using a benchtop OCT system^[25].

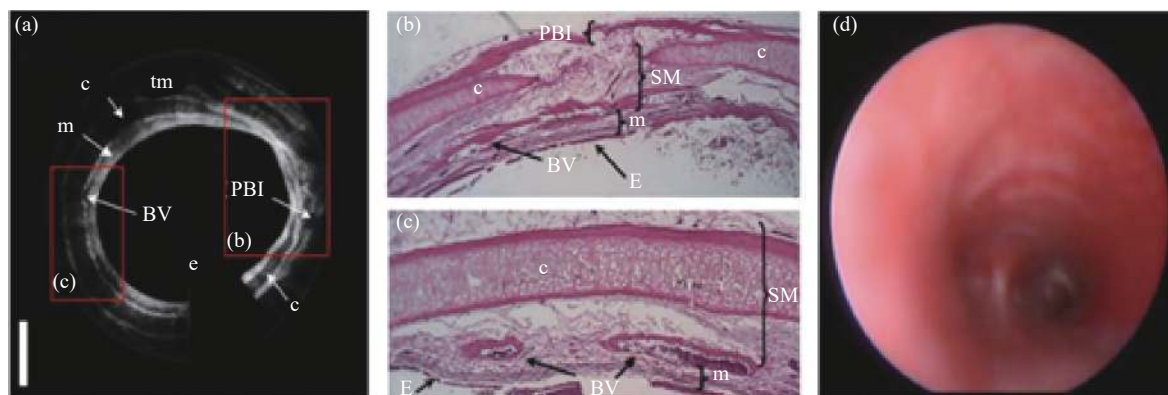


Fig.8 (a) In vivo OCT image of a normal rabbit airway, (b) and (c) histology, and (d) an image of the airway taken by a bronchoscope. (Note: e: epithelium, m: mucosa, c: cartilage, BV: blood vessel, PBT: peri bronchial tissue, and tm: muscularis^[24])

The obtained OCT images closely matched the histologically sectioning. Figure 9 presents the corresponding

histology sections of the scanned macroscopically disease-free airways to validate the OCT images.

1.2 Lung

Diagnostic imaging modalities for human bronchial airways do not possess sufficient resolution and tissue penetration depth to detect early morphologic changes and differentiate real-time neoplastic pathology from nonspecific aberrations^[26]. OCT is a feasible optical tool for real-time near-histologic imaging of endobronchial pathology with the potential for lung cancer surveillance applications in diagnosis and treatment^[27]. And OCT has been shown to be able to evaluate and differentiate pulmonary parenchyma from pulmonary nodules^[14].

In addition, OCT is also a high-resolution imaging modality that rapidly generates helical cross-sectional images. Needle-based OCT to guide Transbronchial Lymph Node Biopsy Transbronchial needle aspiration (TBNA), often used to sample lymph nodes for lung cancer staging, is subject to sampling error even when performed with endobronchial ultrasound^[28]. OCT features of metastatic carcinoma are distinct from benign lymph nodes with micro-architectural features that reflect the morphology of the carcinoma subtype. OCT is also able to distinguish lymph nodes from the adjacent airway wall. OCT imaging of human thoracic lymph nodes demonstrated that needle-based OCT can provide information about lymph node microarchitecture that could be used for intraprocedural TBNA sampling site guidance during lung cancer staging^[28].

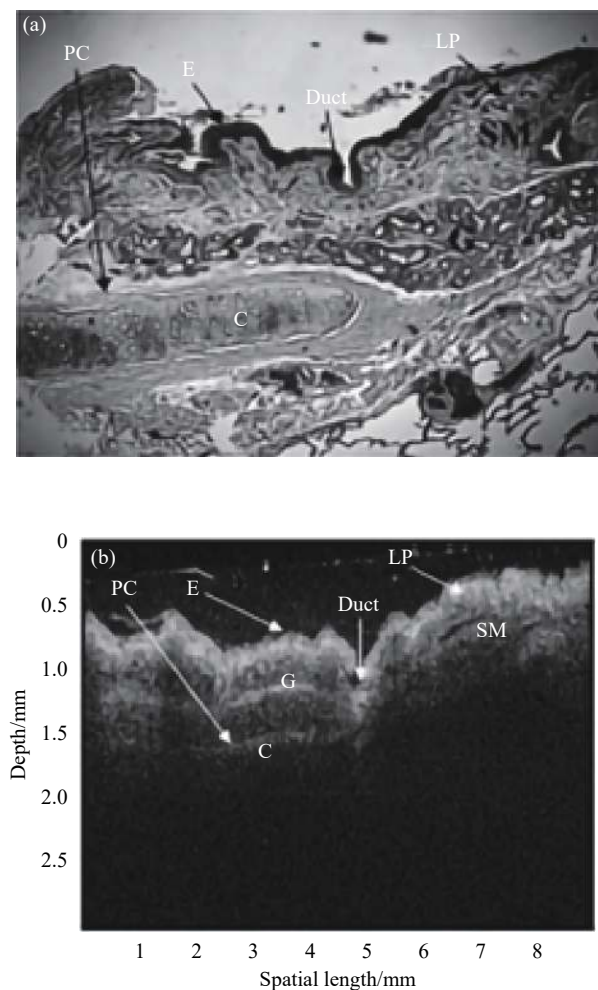


Fig.9 (A) Anatomy of a healthy human airway with its characteristic multilayered profile, (B) Cross-section OCT images in the following anatomic components: Epithelium (E), lamina propria (LP), smooth muscle (SM), mucus glands (G), and cartilage (C)

Diagnostic certainty of idiopathic pulmonary fibrosis (IPF) is critical to determine prognosis and therapeutic options^[29]. OCT can provide unique opportunities to track disease progression, investigate IPF pathogenesis, and assess responses to therapy over time, which would be an asset for both clinical management and research. In vivo OCT also provides strong support for potential significant advances in the management of IPF as it fills the need for low-risk, microscopic evaluation and diagnostic methods that do not require surgery or tissue removal.

Diagnosis and early management of acute respiratory distress syndrome (ARDS) is an unresolved clinical problem in modern burn care. In the new ARDS definition, ARDS is defined as an acute inflammatory syndrome that is accompanied with increased permeability of the alveolar-capillary membrane^[30]. OCT bronchoscopy has the capability to assess changes in Mucosal Thickness (MT) and Proximal Airway Volume (PAV) following smoke inhalation and burns. OCT provides high quality of airway edema information that can be useful in identifying the disease when the patient is exposed to inhalation injury.

OCT has the potential to detect and measure regional changes in mucosal thickness of the airway following smoke inhalation and burns. A bedside technique of fiberoptic-bronchoscopy-based optical coherence tomography (OCT) measurement of airway mucosal thickness (MT) for diagnosis of ARDS following smoke inhalation injury (SII) and burns^[31] may be effective as a diagnostic tool in the early stages of airway damage, smoke inhalation injury and fluid overload after burns.

1.3 Summary of airway and lung

When patients sleep, OCT contributes in the diagnosis of respiratory diseases. OCT is capable of imaging the inside of the respiratory tract. This technology can be used in surgical procedures, and the respiratory tract thickness can also be measured. Researchers require high image resolution and speed. Scientists have designed OCT variants, such as LR-OCT, which have high imaging range. The lung is closely related to the respiratory tract. OCT can solve the diagnosis of many lung diseases and

play the most important role in clinical application.

2 Oral

The application of OCT in the oral cavity includes the detection of oral tissue and cancer. In dentistry, OCT technology can also be used to detect and image patients with dental diseases. The following section reviews the application of OCT technology in the oral cavity.

2.1 Oral tissue

Diseases in human cavities, such as the mouth, are a prevalent and significant health care problem worldwide. Accordingly, the need for an effective diagnostic tool is in high demand for prognosis, diagnosis, and early treatment of cavity diseases^[2]. The characteristic tissue anatomy and micro vessel architecture of various cavity tissue regions of a healthy human are identified by using 3 D OCT images and their corresponding 3 D vascular perfusion maps at a level approaching capillary resolution^[2,32].

A study developed a spectral domain OCT (SD-OCT) system and an oral imaging probe to visualize the microstructural morphology and microvasculature of the human oral cavity^[5], thereby demonstrating the feasibility of microvascular imaging in healthy and pathologic oral tissues.

Recently, the OCT-based microangiography mapping of functional blood flow within tissues has been demonstrated by using a complex OCT processing algorithm, such as the speckle variance method. A study presented the 3 D vascular imaging and clean vascular morphology of living human cavity tissues by using the modified OCT microangiography method^[2].

2.2 Oral cancer

Oral cancer, the sixth most common cancer worldwide, is predominantly seen in low- and middle-income countries^[33]. Violations of the well-defined stratified healthy mucosal structure in cancer tissues are distinctly detected via OCT, thereby indicating the potential of this technique in the early diagnosis of tumors and the precise guidance of excisional biopsy^[34]. However, the use of OCT as a rapid cancer screening technique is limited at present. Therefore, developing a noninvasive and accurate method for real-time screening, detection,

and diagnosis of early-stage oral lesions is still crucial.

A fluorescence image-guided OCT probe could be used on tissue autofluorescence images to simultaneously guide the OCT image acquisition of suspicious regions in real-time. OCT images of normal and precancerous oral mucosae could be used to plot the boundary between the epithelium (EP) and lamina propria (LP) layers reasonably, determine the EP thickness, and estimate the range of dysplastic cell distribution based on standard deviation mapping^[35].

In a study, a mobile OCT imaging system was designed and tested for its performance as a point-of-care

oral diagnostic device in an LMIC^[36]. Another method was used to build a PS-OCT instrument capable of wide-field in vivo imaging in the oral cavity since polarization properties change in cancerous tissue^[37].

2.3 Dental

Dentistry studies on OCT have become an important research direction. An OCT system offered dentists a practical tool for real-time assessment of the remaining dentin thickness on a monitor. OCT could help dentists avoid opening the pulp chamber during dental procedures, such as the drilling process of carries removal^[38]. Figure 10 shows the enface OCT image of the buccal mucosa.

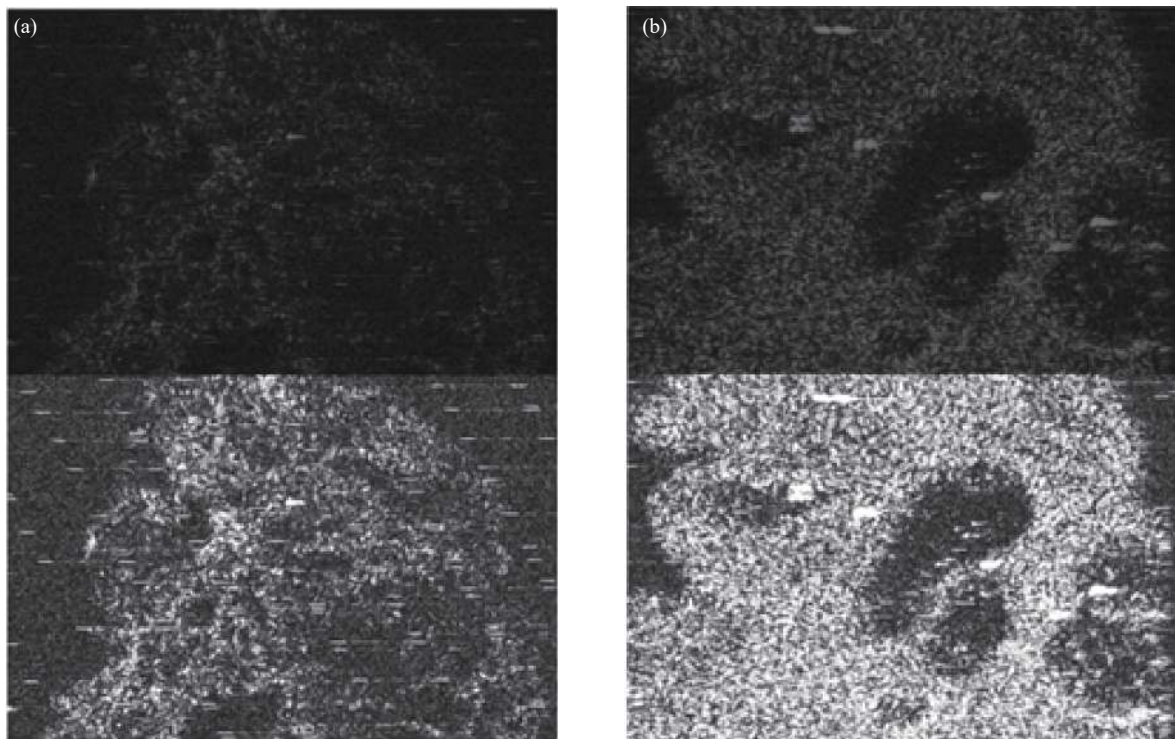


Fig.10 Enface OCT image of the buccal mucosa: (a) healthy tissue and (b) oral squamous cell carcinoma^[38]

2.4 Summary of oral

OCT can also be used for nasal and bronchial disease monitoring. In addition, in the diagnosis of oral diseases, OCT can perform noninvasive and real-time collection of healthy and diseased oral tissues and 3D imaging of blood vessels in the mouth.

3 OCT application in internal organs

In addition to the respiratory tract and oral cavity,

OCT technology can also be used to detect diseases in internal organs, such as kidney, cerebral cortex, skin, bowel and gastric parts.

3.1 Kidney

All OCT and Doppler OCT observations were performed in a noninvasive, sterile, and timely manner on intact human kidneys prior to and following their transplantation^[39]. Providing high-resolution 3D imaging demonstrated the potential of using OCT on image donor

kidney structures and evaluating organ viability or imaging the responses to acute kidney injury^[40]. Moreover, OCT exhibited high diagnostic yield in determining renal cell carcinoma^[41].

For kidney transplants, ischemia-induced acute tubular necrosis (ATN) is the most common complication^[39]. OCT could image the renal microstructures of living human donor kidneys and potentially provide a

measure to determine the extent of ATN. Accurate and early diagnosis is critical in preserving renal function. For delayed diagnosis, acute glomerulonephritis caused by antglomerular basement membrane disease has a high mortality rate^[42]. OCT can detect the difference in tissue properties between healthy and nephritic murine kidneys. [Figure 11](#) shows typical OCT images of healthy and nephritic kidneys.

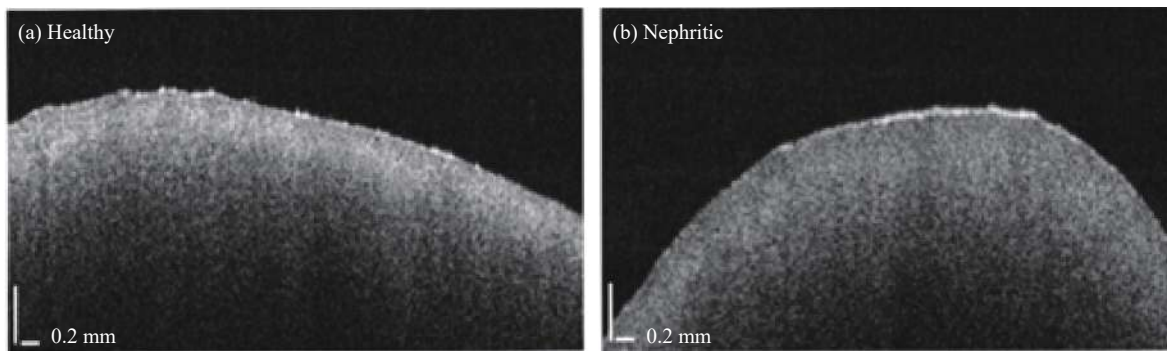


Fig.11 Typical OCT images of (a) healthy and (b) nephritic kidneys^[42]

3.2 Cerebral organs

The accurate quantification of cerebral perfusion from OCT angiograms was important to understand the cerebral vascular pathophysiology^[43]. However, the mechanisms underlying the nontraumatic rupture of cerebral vessels were unclear^[44]. Therefore, quantitative assessment of cerebral blood flow could significantly promote understanding of the nature of acute intracranial hemorrhage (ICH).

A study determined the particularities of alterations in arterial and venous cerebral circulation in hypertensive rats at different stages of stress-related ICH development by using 3D Doppler OCT (D-OCT)^[45]. By using D-OCT, the latent stage of stress-induced ICH was characterized by a decrease in venous outflow.

Moreover, the fractional signal change measured by OCT revealed a functional signal time course corresponding to the hemodynamic signal measurement made with video microscopy^[46]. The results in this study were validated with more than 10 animals to date. However, the quantification of blood vessels from OCT angiography created some current limitations^[42]. Another study

proposed a growing algorithm for a locally adaptive region to solve these problems; this algorithm was also used as an indicator to evaluate the cerebral blood perfusion of middle cerebral artery occlusion in mice. This algorithm could detect micro vessels and ensure good segmentation results for regions with high signals. [Figure 12](#) shows the OCT angiograms of the normal mouse brain and the results of the traditional threshold segmentation algorithm.

A study proposed an algorithm called wavelength dividing multiplexing optical Doppler tomography to effectively enhance the sensitivity of cerebral capillary flow imaging^[47]. A study showed the cerebral artery wall by using OCT, thereby indicating its importance in fluid structure interaction between vessel wall and blood flow^[44]. This study revealed new information on cerebral artery walls. To overcome the obstacles of deflated and collapsed vessels due to missing blood pressure, this study developed a new image processing method and virtual inflation. This work supported the deduction of vessel wall pathologies. [Figure 13](#) shows the ex vivo histology and OCT slice depicting the same vessel part with varying shapes

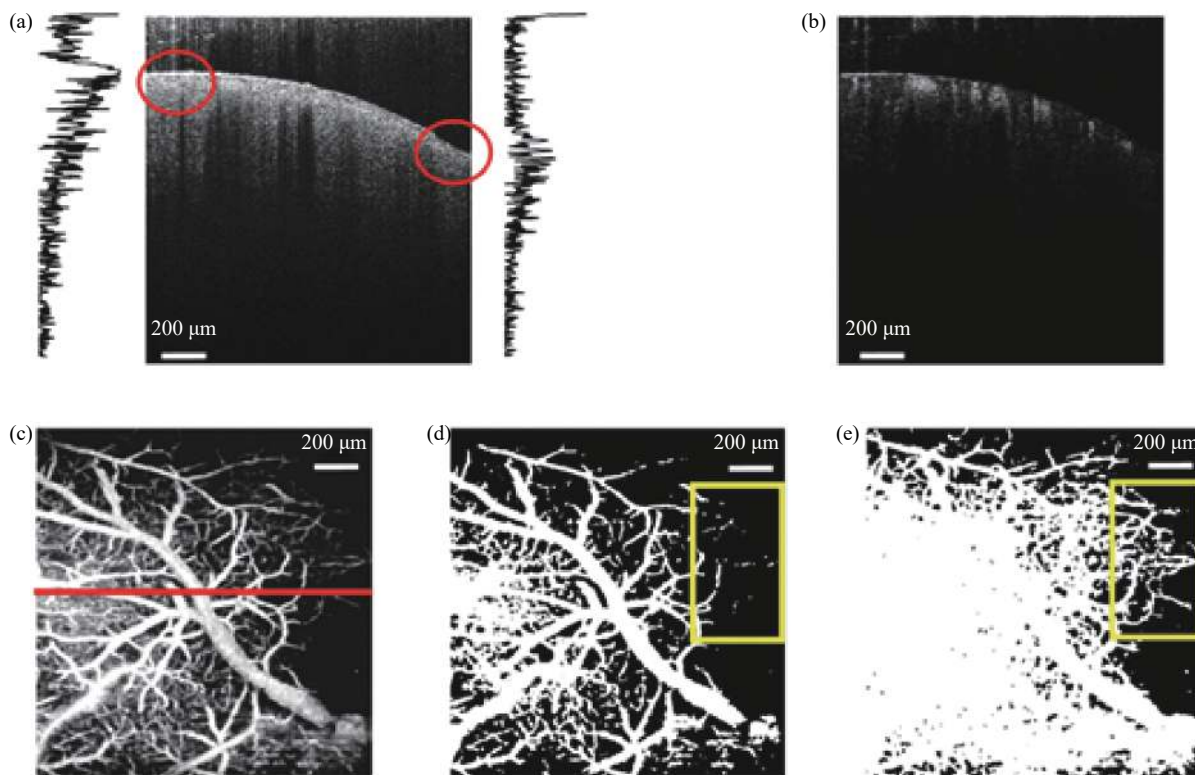


Fig.12 (a) OCT structure image of the mouse brain. [Note: The two red circles indicate that the leftmost and rightmost ends have the maximum and minimum brightness, respectively. The two longitudinal curves next to (a) indicate the signal intensity of the leftmost and rightmost A-scans of (a).] (b) OCT blood flow image of (a). (c) En face MIP image of (b). (Note: The red line represents the locations of (a) and (b).] (d) Segmentation result of the Otsu method. (e) Common threshold segmentation. (Note: The two yellow boxes in (d) and (e) indicate capillaries with relatively lower intensity^[43])

Cerebral edema is the accumulation of excess water in the brain; this condition develops in response to various conditions, including traumatic brain injury and stroke, and contributes to the poor prognosis associated with these injuries^[48]. One study used Doppler OCT techniques to perform 3D imaging of an in vivo water intoxication

model in mice and analyze the cerebral blood flow. This study found that OCT could detect the occurrence of in vivo optical changes. Figure 14 shows that the system was used to image in vivo mouse brain, two-dimensional OCT sagittal image, and 3D volume of in vivo mouse brain.

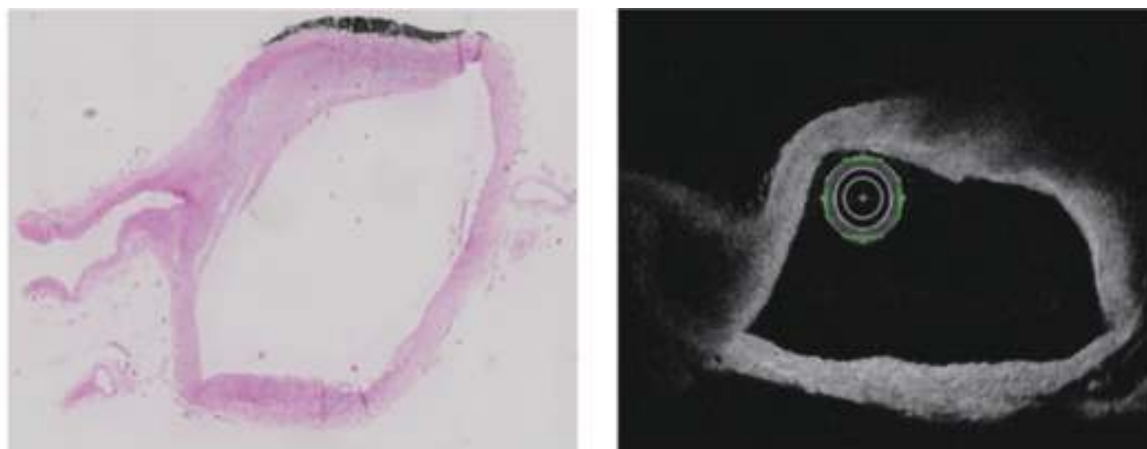


Fig.13 Ex vivo histology and OCT slice depicting the same vessel part with varying shapes^[44]

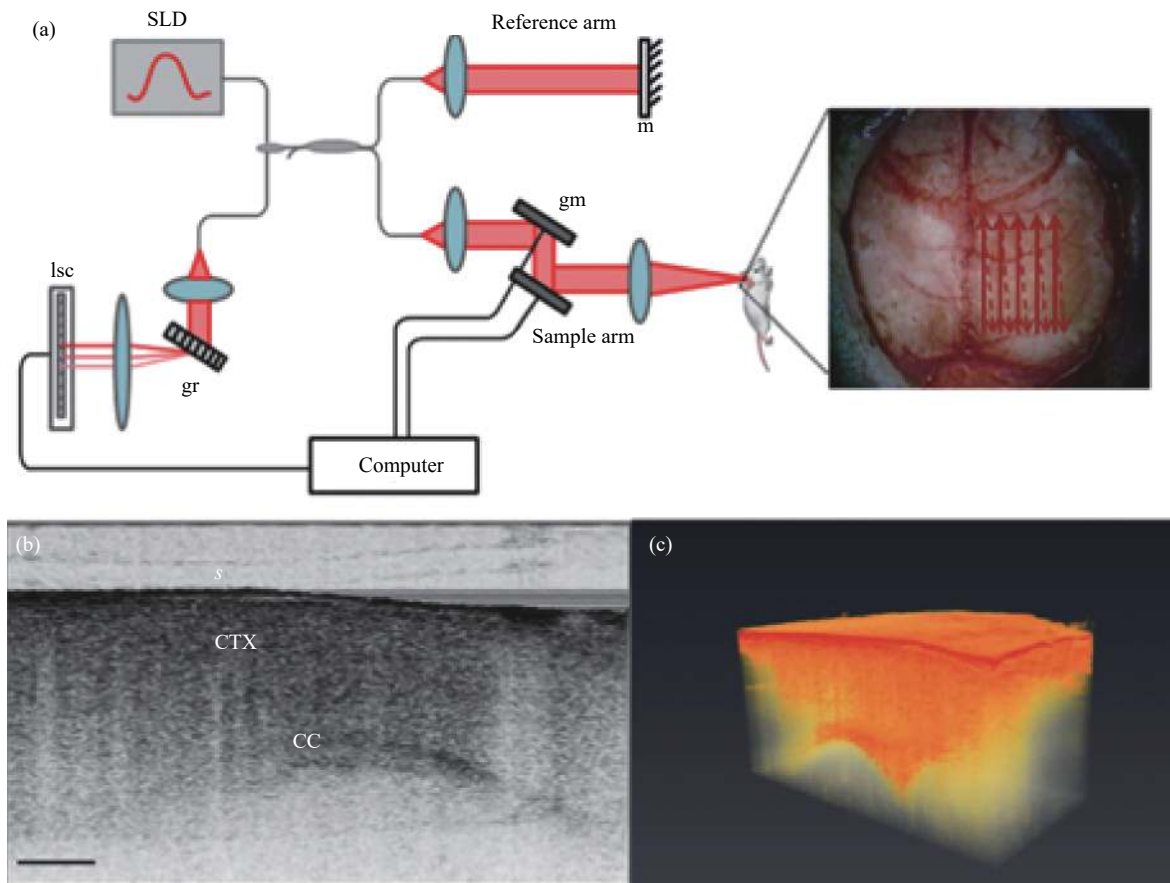


Fig.14 (a) Schematic of the SD-OCT setup; (Note: Red arrows depict the optical beam scan pattern for 3 D imaging of the sample, where m: mirror, gm: galvanometer mounted mirror, gr: grating, lsc: line scan camera).(b) Two-dimensional OCT sagittal image of in vivo mouse brain, where S: skull, CTX: cerebral cortex, CC: corpus callosum, and scale bar: 0.5 mm; (c) 3D volume of in vivo mouse brain rendered from OCT volumetric scan^[48]

3.3 Skin

The skin is the largest organ of the body. This organ has four layers: stratum corneum, epidermis, dermis, and subcutis which have different optical characteristics. Therefore, skin is considered a complex, variable, and multilayered optical medium^[49-50].

OCT could be used as an investigative tool in the clinical evaluation of actinic keratosis and NMSC lesions. A SD-OCT system could detect skin structural imaging by using OCT on healthy skin and different skin lesions, such as dysplasia (AK), Bowen’s disease (BD), and basal cell carcinoma (BCC)^[51].

Furthermore, OCT and Doppler OCT allow rapidly resolved imaging of capillaries in the superficial dermis via a handheld probe to show the morphology^[52]. The vessel morphology and density in the wounded edges

were remarkably different from the healthy skin, showing clusters of glomeruli-like vessels, an absence of linear branching vessels, and substantial blood perfusion.

Another study demonstrated the potential of OCT in providing reliable and quantitative skin surface roughness^[49]. OCT was used to identify the effect of cosmetics and human skin topology on various aging groups and different skin regions. The skin surface geometry obtained from 3D OCT images was well quantified for complex wrinkle structure. Figure 15 shows this procedure.

Vibrational OCT is an emerging technology that characterizes the macromolecular components of the extracellular matrices of the skin^[53]. This method noninvasively identifies the major macromolecular components of skin and scars. Figure 16 shows the cross-sectional OCT images of normal (left) and scarred (right) skin.

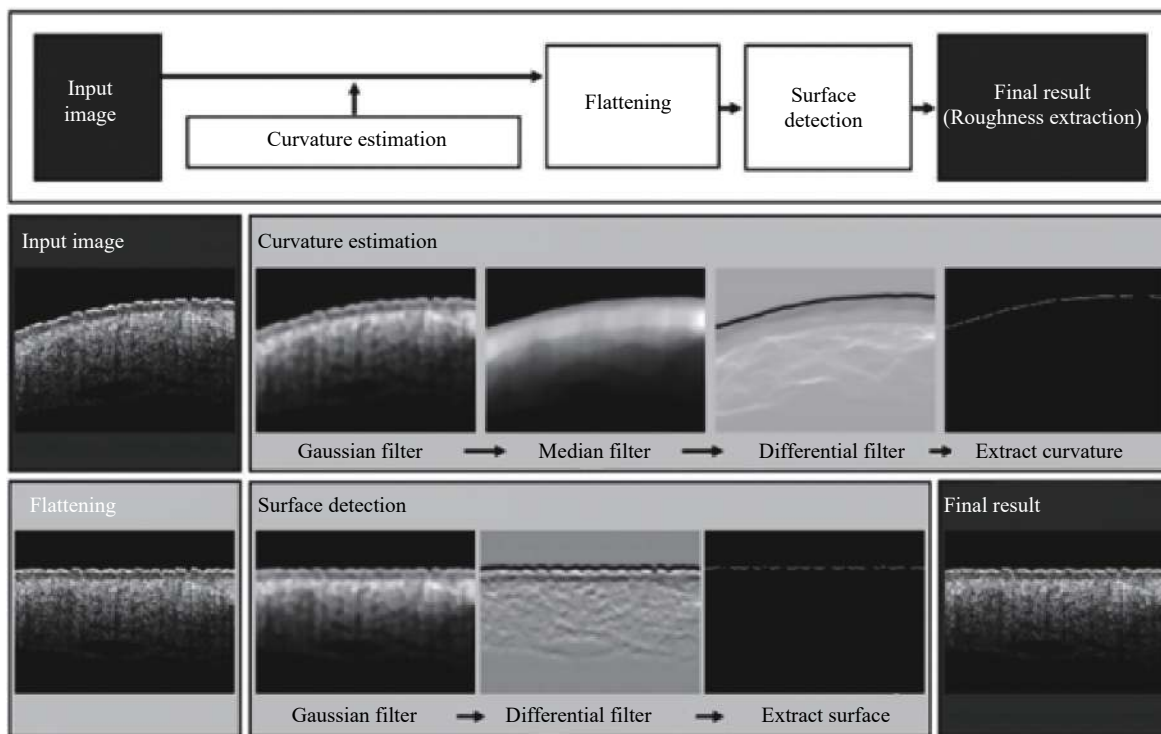


Fig.15 Procedure of the automatic detection algorithm of the skin surface for quantitative analysis of skin roughness. This process includes “curvature estimation” and “surface detection after flattening” procedures^[49]

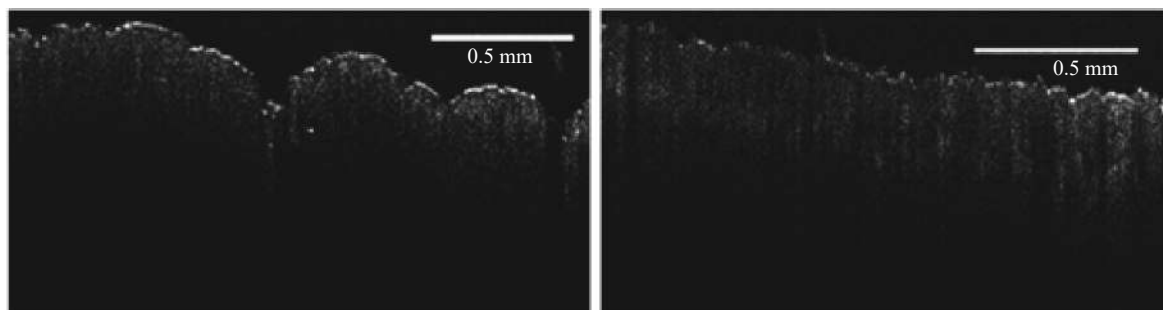


Fig.16 Cross-sectional OCT images of normal (left) and scarred (right) skin^[53]

3.4 Bowel and gastric organs

Anastomotic leakage is a severe complication after esophageal sectioning with gastric tube reconstruction^[54]. Optical modalities indicated the potential in recognizing compromised perfusion in real-time when ischemia is still reversible^[55]. A study investigated an OCT-based intraoperative imaging method for blood flow detection during esophagectomy with gastric tube reconstruction^[56]. By implementing the optical technique for blood flow detection during surgery, perfusion could be imaged and quantified.

The mucosal microanatomy of the large intestine was

characterized by the presence of crypts which were associated predominantly with goblet cells^[57]. These cellular-level intestinal microstructures underwent morphological changes during the progression of bowel diseases, such as colon cancer and ulcerative colitis. Figure 17 presents a cross-sectional image of colon mucosa ex vivo and a representative cross-sectional histology of rat colon tissue.

SD-OCT could be used to image the cellular-level structure in the intestinal mucosa. This method could evaluate OCT for cellular resolution imaging of cellular-level structures in rat colon ex vivo and in vivo. Another

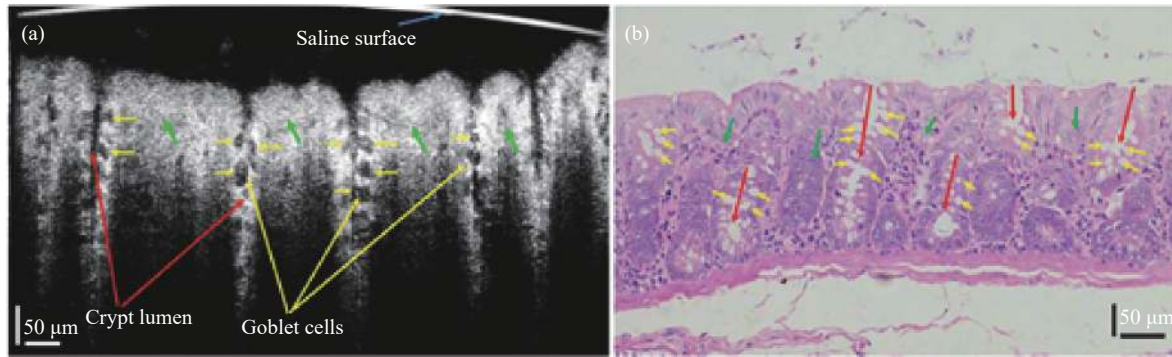


Fig.17 Cross-sectional image of normal rat colon ex vivo. (a) Representative cross-sectional OCT image of colon mucosa ex vivo. (b) Representative cross-sectional histology of rat colon tissue. (Note: The red, yellow, and green arrows denote the crypt lumen structures, individual goblet cells, and lamina propria, respectively^[57])

study demonstrated an ultrahigh-speed endoscopic OCT imaging system for clinical gastroenterology^[58]. This system used next generation tissue visualization methods for clinical gastroenterology that enable 3D visualization of microvasculature.

3.5 Summary of internal organs

OCT can image the cross-section of nerve and blood vessels with high resolution and provide a new model in cerebral cortex neuroscience research to help in solving brain injuries caused by loss of blood pressure in the artery wall vasoconstriction and subsidence problems; thus, OCT can improve vascular blood flow of three-dimensional imaging sensitivity effectively and image the brain edema model. In addition, OCT provides clinicians and researchers with micron-resolution cross-sectional images of the human skin which can be up to several millimeters deep. At present, skin biopsy and the following histopathological analysis are the reference standards for diagnosing skin diseases. OCT is a useful tool to provide comprehensive and intuitive information in dynamic skin observations because it can display quantitative skin topologies and volumetric skin anatomy. In addition, OCT can display microstructures in real time to detect renal cell carcinoma. In addition, SD-OCT can be used to image intestinal mucosal cells, this method is used for imaging the esophageal cavity during gastroscopy to resolve stomach problems.

4 Discussion

This article reviews the applications of OCT in the

diagnosis of different organs, such as OSA, oral cancer, cerebral edema, renal cell carcinoma, and colon cancer in respiratory diseases, oral diseases, brain tissues, renal diseases, and gastrointestinal diseases, respectively.

Traditional X-ray CT is used to obtain airway structure information of patients with respiratory diseases. However, due to the influence of the ionizing radiation dose, X-ray CT cephalometry are limited by time intervals. By contrast, OCT can display respiratory tract in real-time. In order to improve imaging resolution, scientists have developed a variety of OCT, such as aOCT, PS-OCT, SD-OCT, SS-OCT and D-OCT, with high resolution and imaging speed. These methods can also be used to detect lung diseases, and OCT can be used in oral epithelial tissue to determine whether patients have oral cancer and other oral diseases. OCT provides a good tissue image in the clinic. In brain tissues, OCT can detect brain edema, thereby providing doctors with useful information by measuring the thickness of the cerebral artery wall. Lesions in skin tissues can also be measured by using OCT, which has the potential to provide reliable and quantitative skin surface roughness. Colorectal cancer in gastrointestinal diseases and gastric cancer can cause gastrointestinal lesions. OCT can also be used to image gastrointestinal tissues and provide doctors with surgical solutions. As one of the most important organs in the human body, kidneys with renal disease have adverse effects on the human body, and real-time OCT imaging can detect every piece of kidney tissue.

OCT has been used for both quantitative and qualitative morphological evaluations of organ diseases and shown potential as an enabling biophotonic imaging technology for preclinical studies and clinical diagnoses. Hence, the clinical evaluation of diagnostic tests and technologies deserve as much attention as clinical trials investigating new drugs.

References:

- [1] Armstrong Julian, Leigh Matthew, Walton Ian, et al. In vivo size and shape measurement of the human upper airway using endoscopic longrange optical coherence tomography [J]. *Optics Express*, 2003, 11(15): 1817-1826.
- [2] Choi Woo June, Wang Ruikang K. In vivo imaging of functional microvasculature within tissue beds of oral and nasal cavities by swept-source optical coherence tomography with a forward/side-viewing probe [J]. *Biomed Opt Express*, 2014, 5(8): 2620-2634.
- [3] Wijesundara Kushal, Zdanski Carlton, Kimbell Julia, et al. Quantitative upper airway imaging with anatomic optical coherence tomography [J]. *Am J Respir Crit Care Med*, 2006, 173(2): 226-233.
- [4] Davoudi Bahar, Lindenmaier Andras, Standish Beau A, et al. Noninvasive in vivo structural and vascular imaging of human oral tissues with spectral domain optical coherence tomography [J]. *Biomed Opt Express*, 2012, 3(5): 826-839.
- [5] Zysk Adam M, Nguyen Freddy T, Oldenburg Amy L, et al. Optical coherence tomography: A review of clinical development from bench to bedside [J]. *Journal of Biomedical Optics*, 2007, 12(5): 21-30.
- [6] McLaughlin Robert A, Williamson Jonathan P, Phillips Martin J, et al. Applying anatomical optical coherence tomography to quantitative 3 D imaging of the lower airway [J]. *Opt Express*, 2008, 16(22): 17521-17529.
- [7] Ahn Yeh-Chan, Kim Sung Won, Hwang Sang Seok, et al. Optical imaging of subacute airway remodeling and adipose stem cell engraftment after airway injury [J]. *Biomed Opt Express*, 2013, 5(1): 312-321.
- [8] Han S, El-Abbadi N H, Hanna N, et al. Evaluation of tracheal imaging by optical coherence tomography [J]. *Respiration*, 2005, 72(5): 537-541.
- [9] Ridgway, J. M., James Matthew Ridgway, Gurpreet Ahuja, et al. Imaging of the pediatric airway using optical coherence tomography [J]. *Laryngoscope*, 2007, 117(12): 2206-2212.
- [10] Jing J, Zhang J, Loy A C, et al. High-speed upper-airway imaging using full-range optical coherence tomography [J]. *Journal of Biomedical Optics*, 2012, 17(11): 110507.
- [11] Lucey A D, King A J C, Tetlow G A, et al. Measurement, reconstruction, and flow-field computation of the human pharynx with application to sleep apnea [J]. *IEEE Trans Biomed Eng*, 2010, 57(10): 2535-2548.
- [12] Ruofei B, Santosh B, Nicusor I, et al. Airway compliance measured by anatomic optical coherence tomography [J]. *Biomed Opt Express*, 2017, 8(4): 2195-2209.
- [13] Joseph C J, Lidek Chou, Erica Su, et al. Anatomically correct visualization of the human upper airway using a high-speed long range optical coherence tomography system with an integrated positioning sensor [J]. *Sci Rep*, 2016, 6: 39443.
- [14] Sharma G K, Ahuja G S, Wiedmann M, et al. Long-range optical coherence tomography of the neonatal upper airway for early diagnosis of intubation-related subglottic injury [J]. *American Journal of Respiratory and Critical Care Medicine*, 2015, 192(12): 1504-1513.
- [15] Lazarow Frances B, Ahuja Gurpreet S, Chin Loy Anthony, et al. Intraoperative long range optical coherence tomography as a novel method of imaging the pediatric upper airway before and after adenotonsillectomy [J]. *Int J Pediatr Otorhinolaryngol*, 2015, 79(1): 63-70.
- [16] Walsh J H, Leigh M S, Paduch A, et al. Evaluation of pharyngeal shape and size using anatomical optical coherence tomography in individuals with and without obstructive sleep apnoea [J]. *J Sleep Res*, 2008, 17(2): 230-238.
- [17] Leigh Matthew S, Armstrong Julian J, Paduch Alexandre, et al. Anatomical optical coherence tomography for long-term, portable, quantitative endoscopy [J]. *IEEE Trans Biomed Eng*, 2008, 55(4): 1438-1446.
- [18] Wijesundara Kushal, Zdanski Carlton, Kimbell Julia, et al. Quantitative upper airway endoscopy with swept-source anatomical optical coherence tomography [J]. *Biomed Opt Express*, 2014, 5(3): 788-799.
- [19] Volgger Veronika, Sharma Giriraj K, Jing Joseph C, et al. Long-range Fourier domain optical coherence tomography of the pediatric subglottis [J]. *Int J Pediatr Otorhinolaryngol*, 2015, 79(2): 119-126.
- [20] Kirby Miranda, Ohtani Keishi, Nickens Taylor, et al. Reproducibility of optical coherence tomography airway imaging [J]. *Biomed Opt Express*, 2015, 6(11): 4365-4377.
- [21] Adams D C, Hariri L P, Miller A J, et al. Birefringence microscopy platform for assessing airway smooth muscle structure and function in vivo [J]. *Science Translational*

- Medicine*, 2016, 8(359): 359ra131.
- [22] Chou L, Batchinsky A, Belenkiy S, et al. In vivo detection of inhalation injury in large airway using three-dimensional long-range swept-source optical coherence tomography [J]. *Journal of Biomedical Optics*, 2014, 19(3): 036018.
- [23] Qi Li, Huang Shenghai, Heidari Andrew E, et al. Automatic airway wall segmentation and thickness measurement for long-range optical coherence tomography images [J]. *Opt Express*, 2015, 23(26): 33992-34006.
- [24] Lee Sang-Won, Heidary Andrew E, Yoon David, et al. Quantification of airway thickness changes in smoke-inhalation injury using in-vivo 3-D endoscopic frequency-domain optical coherence tomography [J]. *Biomed Opt Express*, 2011, 2(2): 243-254.
- [25] McNichols R J, Ashok Gowda, Brent A. Development of an endoscopic fluorescence image-guided OCT probe for oral cancer detection[C]//Proceedings of SPIE - The International Society for Optical Engineering, 2001, 6(4): 23-30.
- [26] Whiteman Suzanne C, Yang Ying, Gey van Pittius Daniel, et al. Optical coherence tomography: real-time imaging of bronchial airways microstructure and detection of inflammatory/neoplastic morphologic changes [J]. *Clin Cancer Res*, 2006, 12(3Pt1): 813-818.
- [27] Murgu S D, Colt H G. Combined optical coherence tomography and endobronchial ultrasonography for laser-assisted treatment of postintubation laryngotracheal stenosis [J]. *Ann Otol Rhinol Laryngol*, 2013, 122(5): 299-307.
- [28] Shostak E, Hariri L P, Cheng G Z, et al. Needle-based optical coherence tomography to guide transbronchial lymph node biopsy [J]. *Journal of Bronchology & Interventional Pulmonology*, 2018, 25(3): 189-197.
- [29] Hariri L P, Adams D C, Wain J C, et al. Endobronchial optical coherence tomography for low-risk microscopic assessment and diagnosis of idiopathic pulmonary fibrosis in vivo [J]. *American Journal of Respiratory & Critical Care Medicine*, 2017, 197(7): 949-952.
- [30] Miao Y, Choi J H, Chou L D, et al. Automatic proximal airway volume segmentation using optical coherence tomography for assessment of inhalation injury [J]. *Journal of Trauma and Acute Care Surgery*, 2019, 87(1): S132-S137.
- [31] Choi J H, Chou L D, Roberts T R, et al. Point-of-care endoscopic optical coherence tomography detects changes in mucosal thickness in ARDS due to smoke inhalation and burns [J]. *Burns*, 2019, 45(3): S89-S97.
- [32] Sheet D, Banerjee S, Phani S, et al. Transfer learning of tissue photon interaction in optical coherence tomography towards in vivo histology of the oral mucosa[C]//2014 IEEE 11th International Symposium on Biomedical Imaging (ISBI), 2014:1389-1392.
- [33] Ae Heidari, Sunny S P, James B, et al. Optical coherence tomography as an oral cancer screening adjunct in a low resource settings [J]. *IEEE Journal of Selected Topics in Quantum Electronics*, 2019, 25(1): 7202008.
- [34] Sergeev A, Gelikonov V, Gelikonov G, et al. In vivo endoscopic OCT imaging of precancer and cancer states of human mucos [J]. *Optics Express*, 1997, 1(13): 432-440.
- [35] Cheng-Kuang Lee, Ting-Ta Chi, Chiung-Ting Wu, et al. Diagnosis of oral precancer with optical coherence tomography [J]. *Biomed Opt Express*, 2012, 3(7): 1632-1646.
- [36] Nagarajan N, Vasantha J R, Raj J G, et al. A novel design of PCF for supercontinuum source to detect oral cancer using OCT[C]//2015 International Conference on Microwave and Photonics (ICMAP), 2015.
- [37] Amd Lee, Cahill L, Liu K, et al. Wide-field in vivo oral OCT imaging [J]. *Biomed Opt Express*, 2015, 6(7): 2664-2674.
- [38] Sinescu C, Duma V F, Canjau S, et al. Dentistry investigations of teeth and dental prostheses using OCT[C]//SPIE Photonics Europe, 2016.
- [39] Andrews P M, Wang H W, Wierwille J, et al. Optical coherence tomography of the living human kidney [J]. *Journal of Innovative Optical Health Sciences*, 2014, 7(2): 1350064.
- [40] Li Qian, Onozato Maristela, Andrews Peter M, et al. Three-dimensional high-resolution optical coherence tomography (OCT) imaging of human kidney[C]//International Conference of the IEEE Engineering in Medicine & Biology Society, 2009: 5741-5743.
- [41] Buijs Mara, Wagstaff Peter G K, de Bruin Daniel M, et al. An in-vivo prospective study of the diagnostic yield and accuracy of optical biopsy compared with conventional renal mass biopsy for the diagnosis of renal cell carcinoma: The interim analysis [J]. *Eur Urol Focus*, 2018, 4(6): 978-985.
- [42] Chihhao Liu, Yong Du, Manmohan Singh, et al. Combined optical coherence tomography and optical coherence elastography for glomerulonephritis classification[C]//SPIE BiOS, 2016.
- [43] Ma Zhenhe, Ding Ning, Yu Yao, et al. Quantification of cerebral vascular perfusion density via optical coherence tomography based on locally adaptive regional growth [J]. *Appl Opt*, 2018, 57(35): 10117-10124.
- [44] Glaßer S, Hoffmann T, Boese A, et al. Virtual inflation of the

- cerebral artery wall for the integrated exploration of OCT and histology data [J]. *Computer Graphics Forum*, 2017, 36(8): 57-68.
- [45] Oxana V. Semyachkina-Glushkovskaya, Vladislav V. Lychagov, Olga A. Bibikova, et al. The assessment of pathological changes in cerebral blood flow in hypertensive rats with stress-induced intracranial hemorrhage using Doppler OCT: Particularities of arterial and venous alterations [J]. *Photonics and Lasers in Medicine*, 2013, 2(2): 109-116.
- [46] Aguirre A D, Chen Y, Fujimoto J G, et al. Depth-resolved imaging of functional activation in the rat cerebral cortex using optical coherence tomography [J]. *Optics Letters*, 2006, 31(23): 3459-3461.
- [47] Chen W, Du C, Pan Y. Cerebral capillary flow imaging by wavelength-division-multiplexing swept-source optical Doppler tomography [J]. *J Biophotonics*, 2018, 11(8): 201800004.
- [48] Rodriguez C, Szu J I, Eberle M M, et al. Decreased light attenuation in cerebral cortex during cerebral edema detected using optical coherence tomography [J]. *Neurophotonics*, 2014, 1(2): 025004.
- [49] Askaruly S, Ahn Y, Kim H, et al. Quantitative evaluation of skin surface roughness using optical coherence tomography in vivo [J]. *IEEE Journal of Selected Topics in Quantum Electronics*, 2019, 25(1): 7202308.
- [50] Mogensen M, Thrane L, Jørgensen T M, et al. OCT imaging of skin cancer and other dermatological diseases [J]. *Journal of Biophotonics*, 2010, 2(6-7): 442-451.
- [51] Ziolkowska M, Philipp C M, Liebscher J, et al. OCT of healthy skin, actinic skin and NMSC lesions [J]. *Medical Laser Application*, 2009, 24(4): 256-264.
- [52] Holmes J, Schuh S, Bowling F L, et al. Dynamic optical coherence tomography is a new technique for imaging skin around lower extremity wounds [J]. *The International Journal of Lower Extremity Wounds*, 2019, 18(1): 65-74.
- [53] Silver F H, Shah R G. Mechanical spectroscopy and imaging of skin components in vivo: Assignment of the observed moduli [J]. *Skin Res Technol*, 2019, 25(1): 47-53.
- [54] Jansen S M, De B, Van B H M I, et al. Optical techniques for perfusion monitoring of the gastric tube after esophagectomy: A review of technologies and thresholds [J]. *Diseases of the Esophagus Official Journal of the International Society for Diseases of the Esophagus*, 2018, 31(6): 1-11.
- [55] Ji Q, Sudheendran N, Liu C H, et al. Raman spectroscopy complements optical coherent tomography in tissue classification and cancer detection [J]. *Biological Trace Element Research*, 2015, 12: 2078539.
- [56] Sanne M. Jansen, Mitra Almasian, Leah S. Wilk, et al. Feasibility of optical coherence tomography (OCT) for intra-operative detection of blood flow during gastric tube reconstruction [J]. *Sensors (Basel)*, 2018, 18(5): 1331.
- [57] Yu X, Luo Y, Liu X, et al. Towards high speed imaging of cellular structures in rat colon using micro-optical coherence tomography [J]. *IEEE Photonics Journal*, 2016, 8(4): 3900308.
- [58] Tsai Tsung-Han, Lee Hsiang-Chieh, Ahsen Osman O, et al. Ultrahigh speed endoscopic optical coherence tomography for gastroenterology [J]. *Biomed Opt Express*, 2014, 5(12): 4387-4404.